Journal of Materials Chemistry A

Light Induced Coarsening of Metal Nanoparticles

Journal:	*Journal of Materials Chemistry A*
Manuscript ID	TA-ART-11-2018-011341.R1
Article Type:	Paper
Date Submitted by the Author:	08-Apr-2019
Complete List of Authors:	Crozier, Peter; Arizona State University, School for Engineering of Matter, Transport and Energy Liu, Qianlang; Arizona State University, SEMTE Zhang, Luixian ; Arizona State University, School of Mechanical, Aerospace, Chemical and Materials Engineering

Light Induced Coarsening of Metal Nanoparticles

Liuxian Zhang, Qianlang Liu and Peter A. Crozier*

School for Engineering of Matter, Transport and Energy, Arizona State University, Tempe, AZ 85287-6106, USA

*Corresponding author at: crozier@asu.edu

Keywords

Photocatalyst; Pt/TiO_2; Ostwald ripening; Water splitting; Coarsening.

Abstract

We report a novel metal particle coarsening mechanism that is controlled by exposure of the substrate to light. Pt nanoparticles on TiO_2 are observed to undergo enhanced coarsening during light illumination under conditions associated with photocatalytic water splitting. The average Pt particle size changed from 1.7 to 2.1 nm over 12 hours of photoreaction conditions whereas control experiments in the dark showed no change in Pt particle size. The coarsening is thermodynamically driven by the Gibbs-Thompson effect but is kinetically controlled by photon illumination conditions.. These effects accelerate electron transport between particles on the substrate of differing sizes and dramatically increases the rate of Ostwald ripening. This enhanced coarsening mechanism will operate in other metal particle systems supported on semiconductors which harvest light and inject electrons into the conduction band. The kinetic rate of ripening is related to the degree to which the substrate conductivity and photovoltage is enhance during light illumination.

Introduction

Photocatalytic processes are important for energy conversion and remediation of environmental pollutants (Lewis and Nocera 2006, Maeda, Teramura et al. 2006, Kudo and Miseki 2009). Heterogeneous photocatalytic materials are composed of light harvesting semiconductors which are functionalized with metal co-catalysts (Fujishima and Honda 1972, Jakob, Levanon et al. 2003) (Liu, Qu et al. 2004, Sakthivel, Shankar et al. 2004). For example, metal particles such as Pt act as reduction catalysts for adsorbed protons producing hydrogen molecules in water splitting applications (Greeley, Jaramillo et al. 2006). They may also facilitate electron-hole pair separation if the Fermi level of the metal lies below the Fermi or quasi-Fermi level of the oxide semiconductor (Subramanian, Wolf et al. 2001, Anpo and Takeuchi 2003). Long-term stability in aqueous environments remains an ongoing issue for many photocatalysts and photoelectrocatalysts. For example, both the light harvesting semiconducting components (Gerischer 1977, Chen and Wang 2012, Cheng, Benipal et al. 2017) and metal co-catalysts such as Ni are known to photocorrode under reaction conditions (Liu, Zhang et al. 2015, Zhang, Liu et al. 2015, Han, Kreuger et al. 2017). Coarsening processes of Pt nanoparticles on conducting bulk electrodes under electrochemical conditions have also been widely studied in part because of their relevance to fuel cell applications (Ferreira, la O' et al. 2005, Redmond, Hallock et al. 2005, Shao-Horn, Sheng et al. 2007, Shao-Horn, Sheng et al. 2007, Lafforgue, Zadick et al. 2018). The problem of deactivation has motivated fundamental research to elucidate specific kinetic pathways responsible for particle coarsening under a variety of conditions (Wanke and Flynn 1975, Harris 1986, Asoro, Kovar et al. 2010, Simonsen, Chorkendorff et al. 2011, Parthasarathy and Virkar 2013) in order to develop mitigation strategies. Here we describe a photoinduced Ostwald ripening mechanism for supported metal nanoparticles which has not previously been reported.

The current investigation was carried out on the ripening process of supported Pt metal nanoparticles under liquid phase photoreaction conditions. TiO_2 was selected as the light harvesting

support because it is very stable under reaction conditions allowing changes in the behavior of the Pt co-catalyst to be studied. We employed aberration corrected transmission electron microscopy (TEM) to follow the evolution of the particle size distribution during water splitting and observed significant Pt particle coarsening driven by light illumination. Previous work has investigated photodeposition of Pt nanoparticles onto TiO_2 from Pt precursors solutions under UV irradiation(Shironita, Mori et al. 2008). In contrast we explore the changes taking place on Pt nanoparticles already deposited on the support during light and dark conditions. The observed coarsening is interpreted in terms of an Ostwald ripening process which is kinetically controlled by the light induced changes in the TiO_2. The mechanism should be active in other supported metal systems that satisfy the thermodynamic and kinetic conditions described below.

Experiments

Materials Preparation.

2 wt % Pt on high surface area anatase TiO_2 nanoparticles was prepared with a wet chemical impregnation method. A Pt loading of 2 wt% was selected to minimize back reactions and light shadowing by the metal(Ohtani, Iwai et al. 1997, Sayama and Arakawa 1997). The high surface area anatase particles were prepared following a hydrothermal method(Zhang, Miller et al. 2013). The TiO_2 particles were suspended in 20 ml of $PtCl_4$ (Sigma-Aldrich, 99.99%) aqueous solutions, stirred and dried. The particles were then calcined in air @500°C for 3 hrs followed by a reduction in flowing 2% H_2/Ar @500°C for 2 hrs. X-ray diffraction data from the fresh sample is shown in Fig. S1 of the *Supplemental Materials* confirming that the TiO_2 crystal structure is anatase.

Photoreaction Setup

The photoinduced ripening was investigated using a liquid phase photoreaction under UV illumination. 20 mg of the as prepared 2 wt% Pt/TiO_2 material was suspended in 50 ml de-ionized H_2O and a 450W xenon lamp (Newport) fitted with a 350-450 nm bandpass dichroic beam turning

mirror, (which filters out infrared light) was used as the source, with the light coming vertically through the top quartz window of the reactor. The incident light intensity into the reactor was about 50 mW/cm^2 and the temperature increase during the reaction was less than 5°C for the duration of the run. H_2 released during the associated photocatalytic water splitting was constantly swept out of the reactor with Ar as the carrier gas continuously flowing at 5 cc/ min. H_2 was detected and quantified using a gas-chromatography (GC) (Varian 450-GC) system connected to the photoreactor.

Pt Nanoparticles and Solute Characterization.

Pt coarsening during the reaction was characterized with high resolution TEM (HRTEM) on an aberration corrected FEI Titan and high-angle annular dark-field scanning TEM (HAADF STEM) on JEOL 2010F. HAADF was employed to determine accurate Pt particle size distributions at different times during the reaction (Treacy, Howie et al. 1978, Treacy and Rice 1989). During the photoreaction, the reactor was periodically opened to extract small quantities of reactant solution (water and catalyst) for analysis. Pt^{2+} concentrations in solution during the reaction were determined using inductively coupled plasma mass spectrometry (ICP-MS). A series of water samples (2ml each) were taken 1hr, 3hrs, 5hrs, 7hrs and 12 hrs during the photo-reaction from the initial 50ml volume of solution. Photocatalyst particles were separated out efficiently using microsep advance centrifugal devices with omega membranes (Pall Corp.) under 10,200 rpm centrifuges for 15 mins. The water sample after the filtering was acid digested and analyzed by quadrupole ICP-MS (ThermoFisher Scientific iCAP Q, with CCT option). To correlate coarsening observations with photocatalytic activity, a continuous experiment was also run for 12 hours without opening the reactor to follow the H_2 evolution rate.

Results

Morphology and Photocatalytic activity

The morphology of the as prepared 2 wt% Pt on anatase is shown in **Fig.1a**. Pt particles 1-2 nm in size were well dispersed on TiO_2 nanoparticles. Lattice fringes of 2.27 Å were observed on the particles which match the Pt (111) fringe spacings. Most of the Pt particles preferred to nucleate and grow at high surface energy sites including corners and steps as marked on the figure where surface atoms on the TiO_2 support are less coordinated. (TEM imaging of the particles after the reaction still showed 2.27 Å lattice fringes belonging to Pt (111)). The H_2 production rate is plotted in **Fig. 1b** which shows initial transient oscillatory behavior for the first 3 hours followed by a steady drop in H_2 production from about 200 minutes over the subsequent 6 hours. (The initial low H_2 signal is related at least in part to the time it takes for H_2 to reach saturation concentration in water, get released to the head space and then mix fully with Ar carrier gas). *In situ* electron microscopy was also performed in the presence of light and water vapor. These measurements are shown in *Supplemental Materials* and no particle coarsening was observed in the presence of water vapor.

Coarsening of Pt particles

A series of HAADF images were taken on the catalyst after 0 (fresh), 3, 7 and 12 hrs of photo-exposure. Pt particle coarsening is very obvious by comparing the images of the 12 hrs light exposure sample and the initial fresh sample as seen in **Fig. 2** (note images not from same area). Over 300 particle sizes were measured from 15 to 20 images for each sample and particle size distributions were determined. The resulting histograms in **Fig. 3** show the time-dependent particle size increased during light exposure in water. Average particles sizes and surface areas for each sample are summarized in **Table 1**. (The specific surface area (area per unit mass) was estimated

for each sample by dividing the total surface area by the total mass of measured particles (each particle was treated as a hemisphere)).

The average particle size increases from an initial value of 1.69 nm ± 0.05 nm to a final value in 12 hrs of 2.06 nm ± 0.09 nm. (The error is taken to be three times the standard error in the mean). Control experiments in the dark were performed to prove that the observed coarsening is induced by light. The particle size distribution of a sample exposed to liquid water in the dark for 12hrs is compared with a fresh catalyst and the result is shown in **Fig. 4**. The particle size distribution is identical to the fresh sample within experimental error with an average size of 1.66 ± 0.05 nm showing that no detectable coarsening occurred in the dark.

Pt Ion Concentration in Solution during Catalysis

ICP was carried out to measure the time-dependent Pt concentration in solution. Combining the Pt concentration determined by ICP with the mass of fresh catalyst used in the reaction allows the percentage of the Pt ions in solution to be calculated relative to the total mass of Pt. The results are summarized in **Table 2** (in the table 100% is equivalent to 2 wt% Pt). The initial relative concentration of Pt^{2+} in solution is comparatively high, around 1 %, as a result of residual chloride species from the platinum chloride precursor. The Pt concentration drops quickly after the light is turned on because of photo-deposition and reaches less than 0.01% after 5 hours. The photo-deposition of the initial 1% relative concentration of Pt from solution onto the support is too small to explain the observed particle size increase reported in section 3.3. (To increase the mean particle size from 1.7nm to 1.8nm, would require 19% additional mass deposition from solution, which is almost a factor of 20 higher than the initial Pt concentration measured in solution). The concentration of the Pt^{2+} stays low and relatively constant after 5 hours suggesting a dissolution/deposition based kinetic pathway for Pt to transfer from small particles to larger Pt particles.

Discussion

The particle size analysis clearly shows that the Pt nanoparticles are coarsening during exposure to light. We hypothesize that the coarsening mechanism is a photon induced Ostwald ripening process. Ostwald ripening is a particle coarsening process involving thermodynamically less stable small particles that, via kinetic pathways such as surface diffusion, volume diffusion or dissolution/deposition, transform to large particles. The driving force for this is the particle-size dependent chemical potential set by the surface-to-volume ratio of nanoscale particles. From an atomistic view, particles with smaller size have a larger number of under-coordinated atoms so there is a higher probability that these atoms can detach from the particle surface and migrate across a support or dissolve into solution. This leads to a net transfer of atoms from the small particles to the large particles resulting in time-dependent increases in the average particle size. Here we show that, under the conditions employed, it is thermodynamically possible for Pt particles to undergo dissolution. We then discuss how the kinetics of the process is regulated by light illumination of the TiO_2 support.

We focus on the dissolution mechanism for Pt transport. The 5°C temperature difference between the photoreactor and the ambient room (where the dark experiments were performed) is insufficient to thermally drive ripening. The Tamman temperature (traditionally the temperature where thermal ripening occurs) is 750°C so this pathway should be completely shut down at the temperature used for the experiment. We also investigated surface diffusion in light and water vapor using *in situ* electron microscopy (see the Supplemental Materials section). We observed no change in the particle size or distribution even after 11 hours of exposure so, based on this observation, we do not think Pt diffusion across the TiO_2 support is significant.

The initial concentration of Pt detected by ICP and the use of the chloride precursor indicates that there is still some residual $PtCl_4^{2-}$ in solution. A simple thermodynamic analysis shows that dissolution of small Pt particles is possible under such condition with the chloride functioning as an intermediate. As discussed in detail by Tang et al., for a finite-sized single-

component solid of radius *r* in equilibrium with a fluid phase containing that component (e.g., Pt^{2+}/Pt equilibrium), there is a difference in the chemical potentials of the component in the solid and fluid phases given by,

$$\mu_s - \mu_l = (f - \gamma)\Omega(2/r) \qquad \text{Eq (1)}$$

where f is the solid/fluid interface stress (assumed isotropic), γ is the solid/fluid interfacial free energy (assumed isotropic) and Ω is the molar volume of the solid (Tang, Li et al. 2010). For the reaction, $PtCl_4{}^{2-} + 2e^- = Pt + 4Cl^-$, (E=0.755 V., NHE), the chemical potential of Pt in the liquid phase is given by

$$\mu_l = \bar{\mu}_l\left(\overline{PtCl_4}^{2-}\right) + RTln(PtCl_4{}^{2-}/\overline{PtCl_4}^{2-}), \qquad \text{Eq.(2)}$$

where the bar quantity indicates the saturation concentration associated with a planar ($r = \infty$) surface at equilibrium. The chemical potential of the Pt in the solid is given by

$$\mu_s = \bar{\mu}_l\left(\overline{PtCl_4}^{2-}\right) + f_{Pt}\,\Omega_{Pt}(2/r). \qquad \text{Eq.(3)}$$

Using the equilibrium condition of Eq.(1) we obtain,

$$RTln(PtCl_4{}^{2-}/\overline{PtCl_4}^{2-}) = \gamma_{Pt}\Omega_{Pt}(2/r). \qquad \text{Eq.(4)}$$

The left-hand side of this equation is the Gibbs free energy difference for Pt in the liquid phase surrounding a Pt particle of radius *r* and that for a planar surface. Since $\Delta G = -nFE$, (n = number of moles of electrons transferred = 2), we obtain

$$E_{PtCl_4{}^{2-}}(r) = \overline{E}_{Pt Cl_4{}^{2-}} - \gamma_{Pt}\Omega_{Pt}/Fr \qquad \text{Eq.(5)}$$

where $\overline{E}_{Pt Cl_4{}^{2-}}$ is the electric potential for a planar surface; $E_{Pt Cl_4{}^{2-}}(r)$ is the electric potential for a particle with radius *r* surrounded by liquid phase; γ_{Pt} is the surface energy ; Ω_{Pt} is the molar volume of *Pt* and *F* is the Faraday constant(Tang, Li et al. 2010). From our ICP analysis, we

estimate that the concentration of $PtCl_4^{2-}$ is ~ 10^{-7} giving a value of $\overline{E}_{Pt Cl_4{}^{2-}} \sim 0.55V$. Taking $\gamma_{Pt} = 2.4$ Jm^{-2}, $\Omega_{Pt} = 9.09 \times 10^{-6}$ m^3, we obtain

$$E_{PtCl_4{}^{2-}}(r) \sim 0.55 - 0.226/\mathrm{r} \qquad \text{Eq.(6)}$$

where r is in units of nanometers(Diebold 2003). The extra term for small particles compared to the planar surface has a negative shift in the standard electric potential of 0.226/r. The electric potential shift is plotted against particle size in **Fig. 5**. For a 1 nm diameter particle, the potential for initial dissolution of Pt is shifted down by 0.46V giving $E(r) \sim +0.1V$ which is low enough to make initial oxidation of small Pt particles possible. The distributions of the negative potential shifts for each sample can be calculated from the particle size distributions and are plotted in **Fig. 6** for each reaction time. The ripening mechanism impacts the photocatalytic activity in several ways. First, the Pt surface area drops by about 23 % as shown in Table 1. Also the rate of electron transfer to protons will be faster on the small particles compared to the large particles because of the change in potential shown in **Fig**. 5 and 6. Finally the Pt particle number density on the TiO_2 surface decreases which increases the distance that photogenerated electrons have to travel in the TiO_2 to reach the co-catalysts. These factors are considered in more detail in *Supplemental Materials* which shows that the predicted decay in the H_2 production agrees with the experiment (excluding the initial transient period).

This argument and the particle size distributions indicate that, for the conditions employed here, Pt dissolution is thermodynamically possible but it does not give any information about kinetics. The experimental observations show that the rate of coarsening is much faster during illumination. The 5°C temperature difference between experiments performed in the light and the dark is unlikely to cause a large change in kinetics. The temperature increase may cause a small increase in the Pt concentration in solution (see eqn(2)). However, comparing the concentration of Pt in solution (ICP analysis Table 2) with the rate of increase in Pt particle size (Table 2) shows

that these two quantities are not correlated. This suggests that the ripening kinetics is not strongly affected by the Pt solution concentration.

There are several factors which contribute to the acceleration of the ripening during illumination associated with the generation of both photovoltage and photoconductivity in the TiO_2. To understand how kinetics is influenced by illumination conditions, it is important to notice that charge transfer must take place whereby the Pt atoms in the small particle must lose two electrons during dissolution. Conversely, the Pt^{+2} ions in solution must gain two electrons when they incorporate onto the surface of the larger Pt particle. Thus Ostwald ripening via metal dissolution requires a charge compensation path to provide electron transfer between small and large particles. The charge transfer kinetics can be greatly enhanced when the support is a conductor. This is essentially the situation in the fuel cell electrode because the carbon support is an electron conductor. In the current case, the presence or absence of light changes the kinetics of this charge transfer process by changing the conductivity of the underlying TiO_2 support.

In the dark, anatase is a poor conductor with a conductivity of $\sim 10^{-7}\ \Omega^{-1}m^{-1}$ but this increases by 7 orders of magnitude under UV light irradiation (Watanabe, Muramoto et al. 2010, Pomoni, Sofianou et al. 2013). The conductivity and lifetime will vary depending on the incident light intensity and defect densities but greatly enhanced electron transfer will take place under illumination (Fujishima, Zhang et al. 2008). Dissolution of Pt will be inhibited in the dark because charge transfer through the TiO_2 is very slow (see **Fig. 7**). When the catalyst is illuminated with light of energy greater than the TiO_2 bandgap (about 3.2 eV), electron-hole pairs are generated in the TiO_2 putting electrons into the conduction band and holes into the valence band increasing the titania conductivity.

Under illumination, photoexcited electrons accumulate on TiO_2 giving rise to a photovoltage which further drives the ripening. The increased density of electrons in the TiO_2 conduction band cause the quasi-Fermi level of TiO_2 to shift to a more negative electric potential as illustrated in Figure 7 (Subramanian, Wolf et al. 2001). The driving-force/photovoltage of the

electrons to reduce $PtCl_2$- to Pt depends on the electric potential difference between the quasi-Fermi level of TiO_2 and the $PtCl_2$-/Pt redox potential. There is a larger potential difference between the quasi-Fermi level of TiO_2 and the larger Pt particles compared to smaller Pt particles. Thus there's a greater driving force for the larger particles to be reduced which further accelerates the ripening under light illumination.

The overall scheme is summarized in Figure 8. The particle electric potential shift is different for particles of different size leading to a net difference in the electrochemical driving force of:

$$E(\mathrm{r}) - E(\mathrm{R}) = \frac{\gamma_{Pt}\Omega_{Pt}}{nFR} - \frac{\gamma_{Pt}\Omega_{Pt}}{nFr} < 0 \qquad Eq.(7)$$

When small and large particles are connected by the photo-excited conducting TiO_2 substrate, thermodynamically, after partial dissolution, small Pt particles with more negative potential will transfer electrons to large particles. This electron transfer is further enhance the photovoltage generated in the TiO_2. The Pt in the small particles is oxidized and to maintain charge neutrality, Pt^{2+} ions from the small particles travel through the electrolyte to the large particle. Effectively, the two particles behave like the electrodes in a Galvanic cell as described by the schematic drawing in **Fig. 8**. This is similar to the electrochemical coarsening of Ag on conducting substrates reported by Redmond et al (Redmond, Hallock et al. 2005). The difference with the work of Redmond et al is that, in our case, photoconductivity and photovoltage are generated in the TiO_2 during light illumination driving the photoelectrochemical coarsening. The driving force increases as the particle size difference increases. This photo-electrochemical Ostwald ripening process is the mechanism which leads to the observed coarsening of the particle size distribution.

Conclusion

We have observed a novel light induced ripening process for metal particle supported on light sensitive substrates. When Pt/TiO_2 photocatalysts in liquid water are exposed to ultraviolet light, Pt particles undergo accelerated coarsening. High angle annular dark-field imaging was employed to determine the quantitative change in particle size distributions and showed that the average Pt size increased by 20% over 12 hours. Control experiments in the dark showed no change in Pt particle size. Very small concentrations of Pt^{2+} were detected in solution by ICP suggesting the particle size increase is due to an Ostwald ripening process involving dissolution of Pt. In the dark, the TiO_2 substrate is strongly insulating and Ostwald ripening is slowed because charge compensation through the substrate is inhibited. Under light illumination, the conductivity of the TiO_2 is dramatically increased by the injection of electrons into the conduction band enhancing charge compensation through the oxide substrate and driving Pt transport between particles via the liquid phase. The increase in photovoltage during illumination also accelerates the ripening. This enhanced coarsening mechanism will operate in other supported metal photocatalysts which harvest light via photoinduced injection of electrons into the conduction band of a semiconducting component. The kinetics of this process is regulated by changes in the substrate conductivity induced by variations in light illumination.

Acknowledgements

We are grateful to our colleagues at ASU, Profs Candace Chan and Dan Buttry for helpful discussion and also to Prof. Karl Sieradzki for assistance with the electrochemical interpretations of the observations. This work was supported by the U.S. Department of Energy, Office of Science, Basic Energy Sciences, under Award DE-SC0004954. The use of TEM at John M. Cowley Center for High Resolution Microscopy at Arizona State University and the help of Dr. Gwyneth W. Gordon et al from School of Earth and Space Exploration for ICP-MS test at ASU is also gratefully appreciated.

References

Anpo, M. and M. Takeuchi (2003). "The design and development of highly reactive titanium oxide photocatalysts operating under visible light irradiation." Journal of Catalysis **216**(1): 505-516.
Asoro, M. A., D. Kovar, Y. Shao-Horn, L. F. Allard and P. J. Ferreira (2010). "Coalescence and sintering of Pt nanoparticles: in situ observation by aberration-corrected HAADF STEM." Nanotechnology **21**(2): 025701.
Chen, S. Y. and L. W. Wang (2012). "Thermodynamic Oxidation and Reduction Potentials of Photocatalytic Semiconductors in Aqueous Solution." Chemistry of Materials **24**(18): 3659-3666.
Cheng, Q., M. K. Benipal, Q. Liu, X. Wang, P. A. Crozier, C. K. Chan and R. J. Nemanich (2017). "Al2O3 and SiO2 Atomic Layer Deposition Layers on ZnO Photoanodes and Degradation Mechanisms." ACS Applied Materials & Interfaces **9**(19): 16138-16147.
Diebold, U. (2003). "The surface science of titanium dioxide." Surface Science Reports **48**(5–8): 53-229.
Ferreira, P. J., G. J. la O', Y. Shao-Horn, D. Morgan, R. Makharia, S. Kocha and H. A. Gasteiger (2005). "Instability of Pt / C Electrocatalysts in Proton Exchange Membrane Fuel Cells: A Mechanistic Investigation." Journal of The Electrochemical Society **152**(11): A2256-A2271.
Fujishima, A. and K. Honda (1972). "ELECTROCHEMICAL PHOTOLYSIS OF WATER AT A SEMICONDUCTOR ELECTRODE." Nature **238**(5358): 37-+.
Fujishima, A., X. T. Zhang and D. A. Tryk (2008). "TiO_2 Photocatalysis and Related Surface Phenomena." Surface Science Reports **63**(12): 515-582.
Gerischer, H. (1977). "On the stability of semiconductor electrodes against photodecomposition." Journal of Electroanalytical Chemistry and Interfacial Electrochemistry **82**(1–2): 133-143.
Greeley, J., T. F. Jaramillo, J. Bonde, I. B. Chorkendorff and J. K. Norskov (2006). "Computational high-throughput screening of electrocatalytic materials for hydrogen evolution." Nature Materials **5**(11): 909-913.
Han, K., T. Kreuger, B. T. Mei and G. D. Mul (2017). "Transient Behavior of Ni@NiOx Functionalized SrTiO3 in Overall Water Splitting." Acs Catalysis **7**(3): 1610-1614.
Harris, P. J. F. (1986). "The sintering of platinum particles in an alumina-supported catalyst: Further transmission electron microscopy studies." Journal of Catalysis **97**(2): 527-542.
Jakob, M., H. Levanon and P. V. Kamat (2003). "Charge Distribution between UV-Irradiated TiO2 and Gold Nanoparticles: Determination of Shift in the Fermi Level." Nano Letters **3**(3): 353-358.
Kudo, A. and Y. Miseki (2009). "Heterogeneous Photocatalyst Materials for Water Splitting." Chemical Society Reviews **38**(1): 253-278.
Lafforgue, C., A. Zadick, L. Dubau, F. Maillard and M. Chatenet (2018). "Selected Review of the Degradation of Pt and Pd-based Carbon-supported Electrocatalysts for Alkaline Fuel Cells: Towards Mechanisms of Degradation." Fuel Cells **18**(3): 229-238.
Lewis, N. S. and D. G. Nocera (2006). "Powering the planet: Chemical challenges in solar energy utilization." Proceedings of the National Academy of Sciences of the United States of America **103**(43): 15729-15735.
Liu, Q., L. Zhang and P. A. Crozier (2015). "Structure-reactivity relationships of Ni-NiO core-shell co-catalysts on Ta2O5 for solar hydrogen production." Applied Catalysis B: Environmental **172**: 58-64.
Liu, S. X., Z. P. Qu, X. W. Han and C. L. Sun (2004). "A mechanism for enhanced photocatalytic activity of silver-loaded titanium dioxide." Catalysis Today **93-95**: 877-884.

Maeda, K., K. Teramura, D. Lu, T. Takata, N. Saito, Y. Inoue and K. Domen (2006). "Photocatalyst releasing hydrogen from water." Nature **440**: 295.
Ohtani, B., K. Iwai, S.-i. Nishimoto and S. Sato (1997). "Role of Platinum Deposits on Titanium(IV) Oxide Particles: Structural and Kinetic Analyses of Photocatalytic Reaction in Aqueous Alcohol and Amino Acid Solutions." The Journal of Physical Chemistry B **101**(17): 3349-3359.
Parthasarathy, P. and A. V. Virkar (2013). "Electrochemical Ostwald ripening of Pt and Ag catalysts supported on carbon." Journal of Power Sources **234**: 82-90.
Pomoni, K., M. V. Sofianou, T. Georgakopoulos, N. Boukos and C. Trapalis (2013). "Electrical conductivity studies of anatase TiO2 with dominant highly reactive {0 0 1} facets." Journal of Alloys and Compounds **548**: 194-200.
Redmond, P. L., A. J. Hallock and L. E. Brus (2005). "Electrochemical Ostwald Ripening of Colloidal Ag Particles on Conductive Substrates." Nano Letters **5**(1): 131-135.
Sakthivel, S., M. V. Shankar, M. Palanichamy, B. Arabindoo, D. W. Bahnemann and V. Murugesan (2004). "Enhancement of photocatalytic activity by metal deposition: characterisation and photonic efficiency of Pt, Au and Pd deposited on TiO2 catalyst." Water Research **38**(13): 3001-3008.
Sayama, K. and H. Arakawa (1997). "Effect of carbonate salt addition on the photocatalytic decomposition of liquid water over Pt-TiO2 catalyst." Journal of the Chemical Society-Faraday Transactions **93**(8): 1647-1654.
Shao-Horn, Y., W. C. Sheng, S. Chen, P. J. Ferreira, E. F. Holby and D. Morgan (2007). "Instability of Supported Platinum Nanoparticles in Low-Temperature Fuel Cells." Topics in Catalysis **46**(3): 285-305.
Shao-Horn, Y., W. C. Sheng, S. Chen, P. J. Ferreira, E. F. Holby and D. Morgan (2007). "Instability of supported platinum nanoparticles in low-temperature fuel cells " Topics in Catalysis **46**: 285-305.
Shironita, S., K. Mori, T. Shimizu, T. Ohmichi, N. Mimura and H. Yamashita (2008). "Preparation of nano-sized platinum metal catalyst using photo-assisted deposition method on mesoporous silica including single-site photocatalyst." Applied Surface Science **254**(23): 7604-7607.
Simonsen, S. B., I. Chorkendorff, S. Dahl, M. Skoglundh, J. Sehested and S. Helveg (2011). "Ostwald ripening in a Pt/SiO2 model catalyst studied by in situ TEM." Journal of Catalysis **281**(1): 147-155.
Subramanian, V., E. Wolf and P. V. Kamat (2001). "Semiconductor−Metal Composite Nanostructures. To What Extent Do Metal Nanoparticles Improve the Photocatalytic Activity of TiO2 Films?" The Journal of Physical Chemistry B **105**(46): 11439-11446.
Tang, L., X. Li, R. C. Cammarata, C. Friesen and K. Sieradzki (2010). "Electrochemical Stability of Elemental Metal Nanoparticles." Journal of the American Chemical Society **132**(33): 11722-11726.
Treacy, M. M. J., A. Howie and C. J. Wilson (1978). "Z-contrast of platinum and palladium catalysts." Philosophical Magazine A **38**(5): 569-585.
Treacy, M. M. J. and S. B. Rice (1989). "Catalyst Particle Sizes from Rutherford Scattered Intensities." Journal of Microscopy **156**: 211-234.
Wanke, S. E. and P. C. Flynn (1975). "The Sintering of Supported Metal Catalysts." Catalysis Reviews **12**(1): 93-135.
Watanabe, Y., Y. Muramoto and N. Shimizu (2010). Electronic properties of TiO2 thin films under UV light irradiation. Electrical Insulation and Dielectric Phenomena (CEIDP), 2010 Annual Report Conference on.
Zhang, L., Q. Liu, T. Aoki and P. A. Crozier (2015). "Structural Evolution During Photocorrosion of Ni/NiO Core/Shell Co-Catalyst on TiO2 " Journal of Physical Chemistry C **119**: 7207-7214.

Zhang, L. X., B. K. Miller and P. A. Crozier (2013). "Atomic Level In Situ Observation of Surface Amorphization in Anatase Nanocrystals During Light Irradiation in Water Vapor." Nano Letters **13**(2): 679-684.

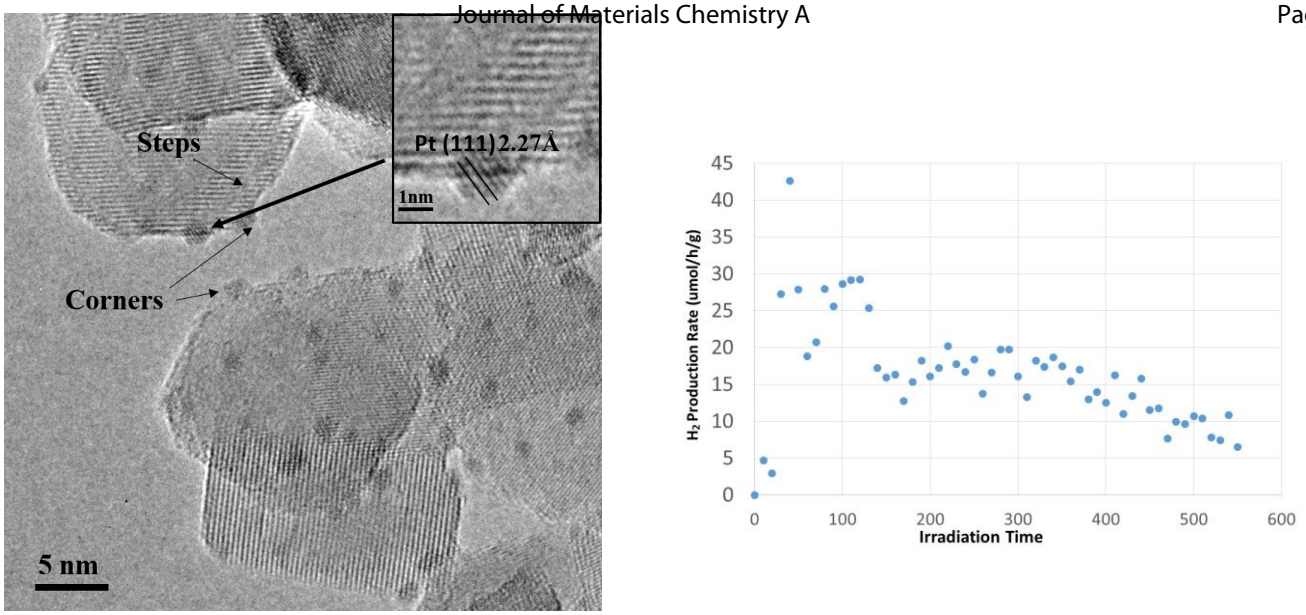

Fig. 1. **a)** TEM image of as prepared 2 wt% Pt/TiO_2 showing good dispersion of 1~2nm Pt particles. Pt particles prefer to nucleate at high surface energy sites such as surface corners and steps. **b)** Steady state H_2 evolution rate per gram of catalysts vs light irradiation time in minutes.

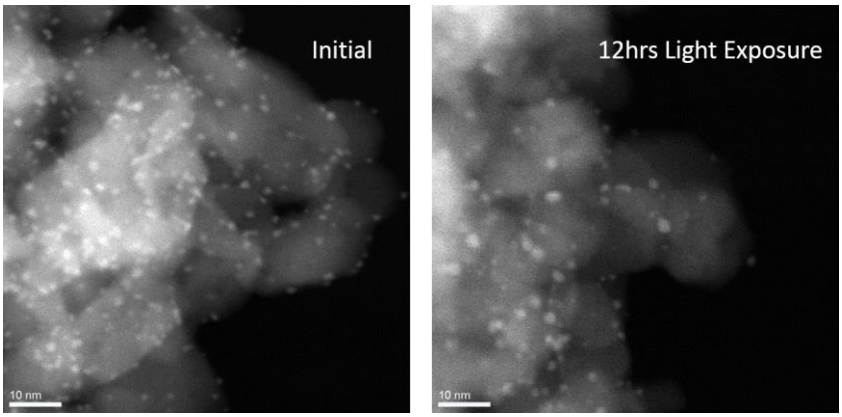

Fig. 2. HAADF-STEM image of a) initial sample and b) after 12hrs light exposure in H_2O.

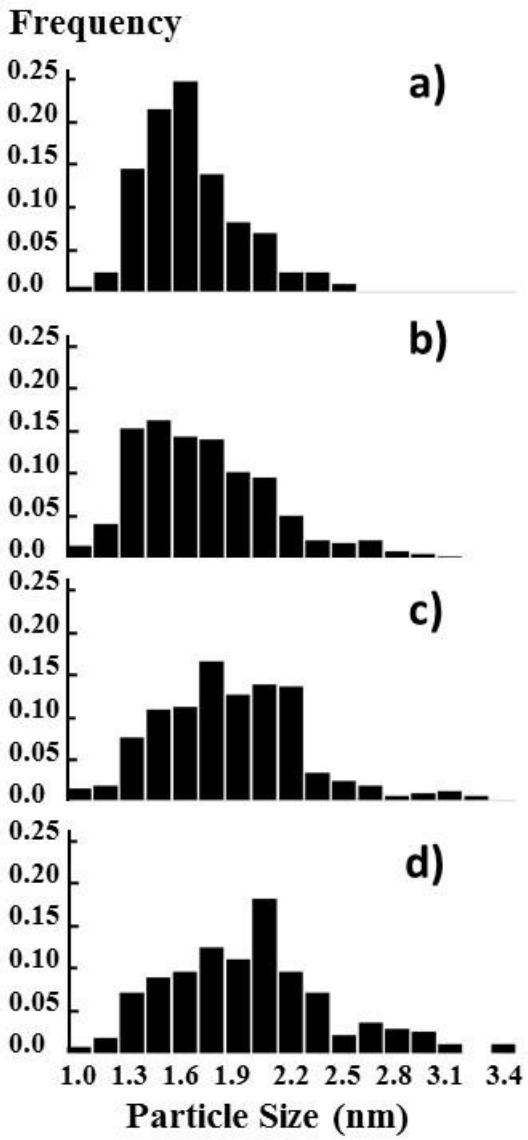

Fig. 3. Particle distribution of samples after different irradiation times for a) fresh b) 3 hours c) 7 hours and d) 12 hours.

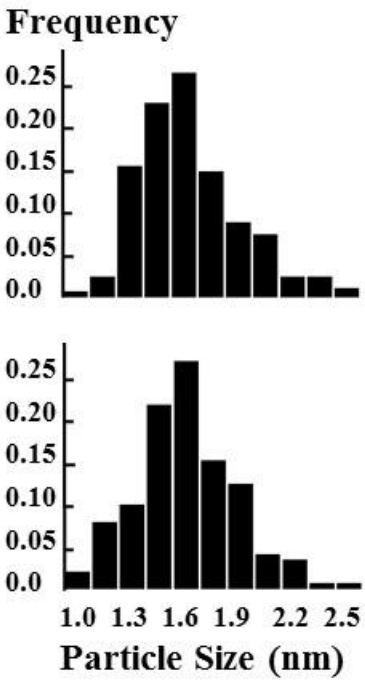

Fig. 4. Particle size distribution of fresh sample and sample after 12hrs in H_2O in dark. No coarsening was observed on samples in dark.

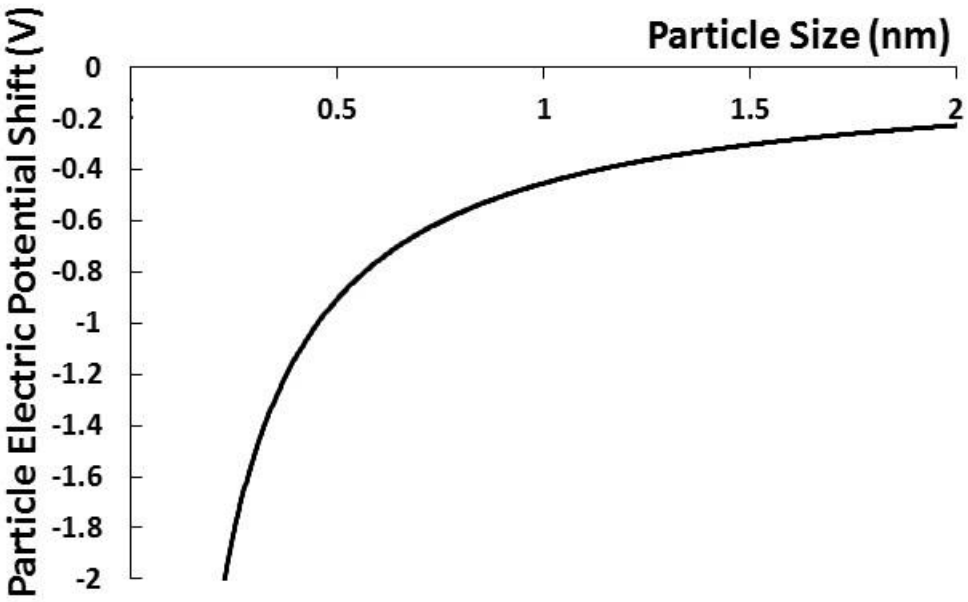

Fig. 5. Particle electric potential shift as a function of particle diameter (taken from eqn(6)).

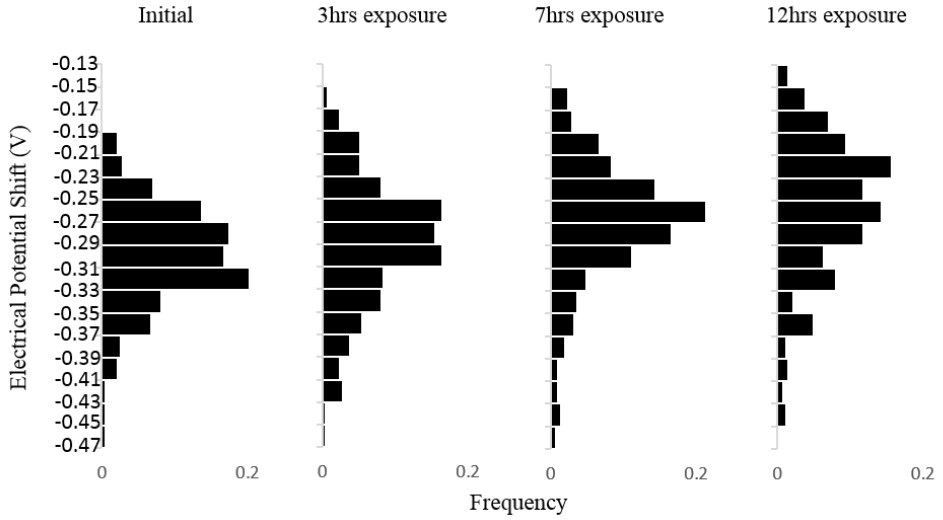

Fig. 6. Electrode potential shift distribution of samples after different irradiation times.

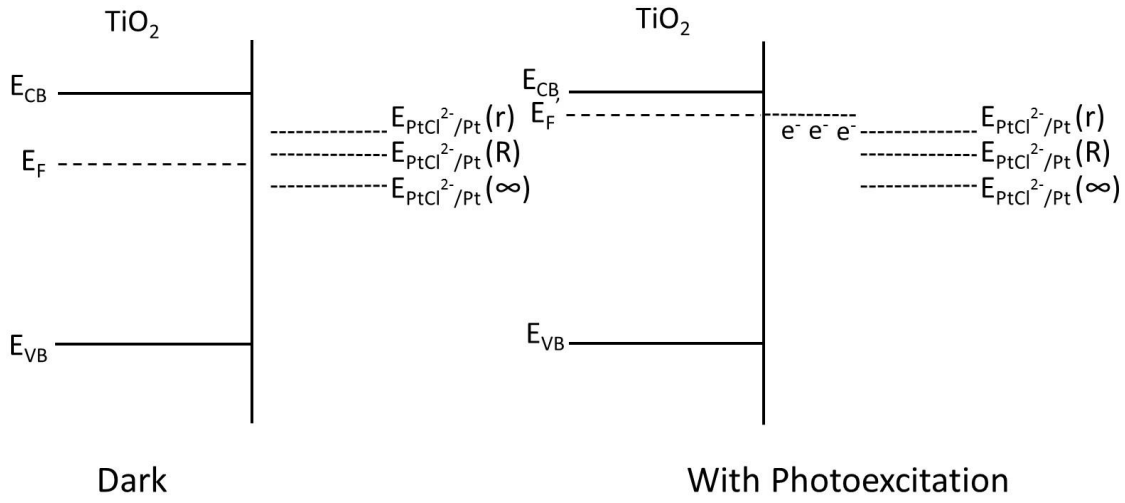

Fig. 7. Schematic drawing of negative shift of quasi-fermi level of TiO_2 particles during photoexcitation.

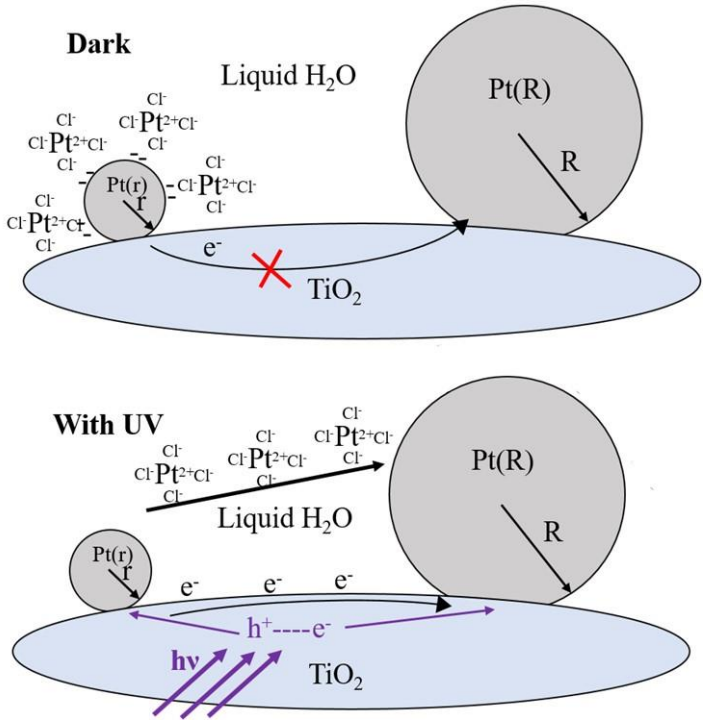

Fig. ~~7~~8. Schematic ~~drawing~~ summary of photo-electro-chemical Ostwald ripening progress. In the dark (upper) negligible dissolution happens because of slow electron transport. During illumination (lower), the TiO_2 becomes conducting connecting small and large Pt particles. Charge transport through the TiO_2 compensates for ion transport through the water accelerating Ostwald ripening.

Table 1. Average particle sizes and specific surface areas during different time periods of irradiation. The surface area dropped by a factor of 1.3 after 12hrs irradiation.

	fresh	3hrs	7hrs	12hrs	12hrs Dark
average particles size (nm)	1.69±0.05	1.77±0.07	1.93±0.07	2.06±0.09	1.66+0.05
surface area (m^2/g)	157	144	133	121	155

Table 2. Pt^{2+} concentration in H_2O during different time periods of light irradiation. The as-prepared sample contains Pt^{2+} from precursors not fully reduced to Pt metal. The initial Pt^{2+} concentration drops because of photo-deposition onto TiO_2 when exposed to light. The Pt^{2+} concentration stays very low because Pt^{2+} redeposits onto large Pt particles after dissolution from small ones.

Irradiation Time	Pt^{2+} Concentration (ppb)	% of Pt dissolved into H_2O
Initial	114.47	1.43%
1 hour	6.88	0.08%
3 hour	3.99	0.05%
5 hour	0.36	below 0.01%
7 hour	0.50	below 0.01%
12 hour	1.21	below 0.01%

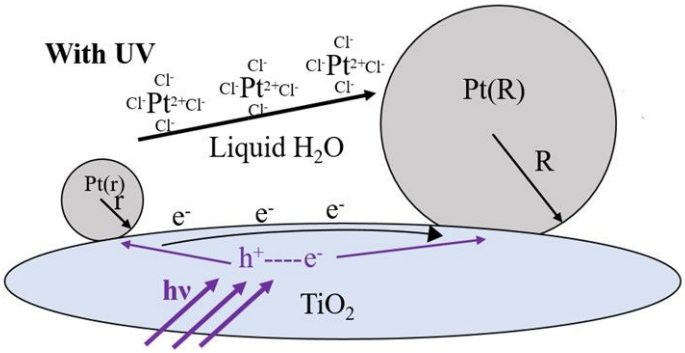

Metal particle coarsening driven by light illumination of the supporting semiconducting substrate.